American Journal of Pathology, Vol. 156, No. 5, May 2000

Vascular Endothelial Growth Factor (VEGF)-Induced Retinal Vascular Permeability Is Mediated by Intercellular Adhesion Molecule-1 (ICAM-1)

Kazuaki Miyamoto,*† Samer Khosrof,*† Sven-Erik Bursell,‡ Yasufumi Moromizato,*† Lloyd Paul Aiello,‡ Yuichiro Ogura,§ and Anthony P. Adamis*†

From the Laboratory for Surgical Research, Children's Hospital, Harvard Medical School, Boston, Massachusetts; the Department of Ophthalmology,† Massachusetts Eye and Ear Infirmary, Harvard Medical School, Boston, Massachusetts; the Department of Ophthalmology,‡ Joslin Diabetes Center, Harvard Medical School, Boston, Massachusetts; and the Department of Ophthalmology,§ Nagoya City University Medical School, Nagoya, Japan*

Two prominent vascular endothelial growth factor (VEGF)-induced retinal effects are vascular permeability and capillary nonperfusion. The mechanisms by which these effects occur are not completely known. Using a rat model, we show that intravitreous injections of VEGF precipitate an extensive retinal leukocyte stasis (leukostasis) that coincides with enhanced vascular permeability and capillary nonperfusion. The leukostasis is accompanied by the up-regulation of intercellular adhesion molecule-1 expression in the retina. The inhibition of intercellular adhesion molecule-1 bioactivity with a neutralizing antibody prevents the permeability and leukostasis increases by 79% and 54%, respectively. These data are the first to demonstrate that a nonendothelial cell type contributes to VEGF-induced vascular permeability. Additionally, they identify a potential mechanism for VEGF-induced retinal capillary nonperfusion. ***(Am J Pathol 2000, 156:1733–1739)***

In experimental diabetes, the increased presence of static leukocytes in the retinal circulation is correlated with increased vascular permeability.[1] The leukostasis and vascular permeability changes coincide with the up-regulation of retinal intercellular adhesion molecule-1 (ICAM-1). When ICAM-1 bioactivity is blocked with an antibody, the retinal leukostasis and vascular permeability increases are reduced by 49% and 86%, respectively.[1]

When the retina is bathed in pathophysiological concentrations of vascular endothelial growth factor (VEGF), enhanced vascular permeability and capillary nonperfusion are among the vascular changes induced.[2–4] The mechanisms by which these changes occur are largely unknown.

The current studies examined the mechanisms underlying VEGF-induced retinal permeability and nonperfusion. Previous work has shown that ICAM-1 and VEGF levels are increased in the diabetic retinae of humans and rodents.[1,5–7] Given the ability of VEGF to increase ICAM-1 expression in the retinal vasculature,[8] the role of ICAM-1 in VEGF-induced vascular permeability and nonperfusion was examined *in vivo*. Our results demonstrate that the VEGF-induced changes are mediated, in part, via the adhesion of leukocytes to ICAM-1.

Materials and Methods

Animals

All experiments were performed in accordance with the Association for Research in Vision and Ophthalmology Statement for the Use of Animals in Ophthalmic and Vision Research and were approved by the Animal Care and Use Committees of the Children's Hospital and Joslin Diabetes Center. Long-Evans rats weighing approximately 200 g were used for these experiments. They were allowed free access to food and water in an air-conditioned room with a 12-hour light/12-hour dark cycle until they were used for the experiments.

Intravitreous Injection Procedure

The rats were anesthetized with xylazine hydrochloride (4 mg/kg; Phoenix Pharmaceutical, St. Joseph, MO) and ketamine hydrochloride (25 mg/kg; Parke-Davis, Morris Plains, NJ). Intravitreous injections were performed by inserting a 30-gauge needle into the vitreous at a site 1 mm posterior to the limbus of the eye. Insertion and infusion were performed and directly viewed through an operating microscope. Care was taken not to injure the

Supported by the Roberta W. Siegel Fund, the Juvenile Diabetes Foundation, the National Eye Institute (R01 EY12611 and EY11627), and a Massachusetts Lions Eye Research Fund grant.

Accepted for publication January 28, 2000.

K. M. and S. K. contributed equally to this work.

Address reprint requests to Anthony P. Adamis, Massachusetts Eye and Ear Infirmary, 243 Charles Street, Boston, MA 02114. E-mail: adamis@hub.tch.harvard.edu.

lens or the retina. The tip of the needle was positioned over the optic disk, and a 5-μl volume was slowly injected into the vitreous. Any eyes that exhibited damage to the lens or retina were discarded and not used for the analyses.

Acridine Orange Leukocyte Fluorography (AOLF) and Fluorescein Angiography

Leukocyte dynamics were evaluated using AOLF.[9,10] Intravenous injection of acridine orange causes leukocytes and endothelial cells to fluoresce through the noncovalent binding of the molecule to double-stranded nucleic acid. When a scanning laser ophthalmoscope is used, retinal leukocytes and blood vessels can be visualized *in vivo*. Twenty minutes after acridine orange injection, static leukocytes in the capillary bed, if present, can be observed.

Twenty-four hours before leukocyte dynamics were observed, a heparin-lock catheter was surgically implanted in the right jugular vein for the administration of acridine orange and sodium fluorescein dye. The catheter was subcutaneously externalized to the back of the neck. The rats were anesthetized for this procedure with xylazine hydrochloride (4 mg/kg) and ketamine hydrochloride (25 mg/kg).

Immediately before AOLF, each rat was again anesthetized, and the pupil of the left eye was dilated with 1% tropicamide (Alcon, Humancao, PR) to observe leukocyte dynamics. A focused image of the peripapillary fundus of the left eye was obtained with a scanning laser ophthalmoscope (Rodenstock Instrument, Munich, Germany). Acridine orange (Sigma, St. Louis, MO) was dissolved in sterile saline (1.0 mg/ml) and 3 mg/kg was injected through the jugular vein catheter at a rate of 1 ml/minute. The fundus was observed with the scanning laser ophthalmoscope using the argon blue laser as the illumination source and the standard fluorescein angiography filter in the 40° field setting for 1 minute. Twenty minutes later, the fundus was again observed to evaluate retinal leukostasis. The images were recorded on videotape at the rate of 30 frames/second. The recordings were analyzed on a computer equipped with a video digitizer (Radius, San Jose, CA) that digitizes video images in real time (30 frames/second) at 640 × 480 pixels with an intensity resolution of 256 steps. For evaluating retinal leukostasis, an observation area around the optic disk measuring five disk diameters in radius was outlined by drawing a polygon bordered by the adjacent major retinal vessels. The area was measured in pixels and the density of trapped leukocytes was calculated by dividing the number of static leukocytes, which were recognized as fluorescent dots, by the area of the observation region. A leukocyte was considered static if its position did not change for 3 minutes. The density of leukocytes was calculated in 8 peripapillary observation areas and an average density was obtained by averaging the 8 density values (1 μm = 3.2 pixels).

Immediately after observing and recording the static leukocytes, fluorescein angiography was performed to study the relationship between static leukocytes and the retinal vasculature. Twenty microliters of 1% sodium fluorescein was injected into the jugular vein catheter and the images were captured using the scanning laser ophthalmoscope as described above.

Quantitation of Retinal ICAM-1 mRNA Levels

Retinas were gently dissected free and cut at the optic disk immediately after enucleation and frozen in liquid nitrogen. Total RNA was isolated from rat retinas according to the acid guanidinium thiocyanate-phenol-chloroform extraction method. A 425-bp *Eco*RI/*Bam*HI fragment of rat ICAM-1 cDNA was prepared by reverse transcription-polymerase chain reaction. The polymerase chain reaction product was cloned into pBluescript II KS vector. After linearization by digestion with *Eco*NI, transcription was performed with T7 RNA polymerase in the presence of [^{32}P]dUTP, generating a 225-bp riboprobe. An automated DNA sequencer verified the sequence of the cloned cDNA. Ten micrograms of total cellular RNA was used for the ribonuclease protection assay. All samples were simultaneously hybridized with an 18S riboprobe (Ambion, Austin, TX) to normalize for variations in loading

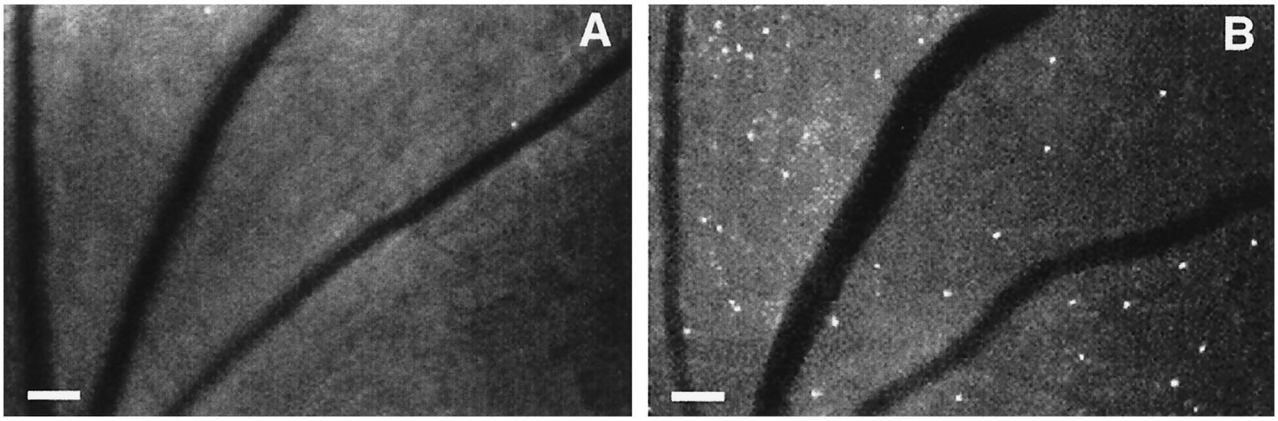

Figure 1. VEGF-induced retinal leukostasis. **A:** AOLF appearance of a normal retinal before injection of 50 ng VEGF. **B:** AOLF appearance of the same retinal area 48 hours after intravitreous VEGF injection. Numerous static leukocytes are visible (white dots), as well as vessel dilation and tortuosity. Mobile leukocytes are not visible in this phase of the study. Scale bar, 100 μm (3.2 pixels = 1 μm).

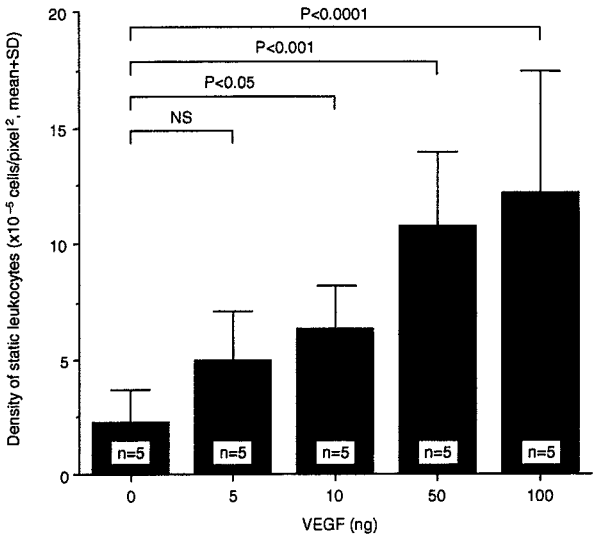

Figure 2. Dose-response graph of VEGF-induced retinal leukostasis. The indicated amount of VEGF was delivered via intravitreous injection and leukostasis was quantitated with AOLF 48 hours later.

and recovery of RNA. Protected fragments were separated on a gel of 5% acrylamide, 8 mol/L urea, 1× Tris-borate-EDTA, and quantified with a PhosphorImager (Molecular Dynamics, Sunnyvale, CA).

Quantitation of Retinal Vascular Permeability

Vascular leakage was quantified using the isotope dilution technique.[11] Briefly, purified monomer bovine serum albumin (BSA; 1 mg, Sigma, St. Louis, MO) was iodinated with 1 mCi of ^{131}I or ^{125}I using the iodogen method. Polyethylene tubing (0.58 mm internal diameter) was used to cannulate the right jugular vein and the left or right iliac artery. The tubing was filled with heparinized saline (400 U heparin/ml). The right jugular vein cannula was used for tracer injection. The iliac artery cannula was connected to a 1-ml syringe attached to a Harvard Bioscience model PHD 2000 constant withdrawal pump preset to withdraw at a constant rate of 0.055 ml/minute. At time 0, [^{125}I] albumin (50 million cpm in 0.3 ml saline) was injected into the jugular vein and the withdrawal pump started. At the 8-minute mark, 0.2 ml (50 million cpm in 0.3 ml saline) of [^{131}I] BSA was injected into the jugular vein. At the 10-minute mark, the heart was excised, the withdrawal pump was stopped, and the retina was quickly dissected and sampled for γ-spectrometry. Tissue and arterial samples were weighed and counted in a γ-spectrometer (Beckman 5500, Irvine, CA). The data were corrected for background and a quantitative index of [^{125}I] tissue clearance was calculated as previously described[11] and expressed as μg plasma × g tissue wet weight^{-1} × minutes^{-1}. Briefly, [^{125}I] BSA tissue activity was corrected for [^{125}I] BSA contained within the tissue vasculature by multiplying [^{125}I] BSA activity in the tissue by the ratio of [^{125}I] BSA/[^{131}I] BSA in an arterial plasma sample. The vascular-corrected [^{125}I] BSA activity was divided by the time-averaged [^{125}I] BSA plasma activity (obtained from a well-mixed sample of plasma taken from the withdrawal syringe) and by the tracer circulation time (10 minutes) and then normalized per gram tissue wet weight.

Anti-ICAM-1 Antibody Inhibition of Retinal Vascular Permeability and Leukostasis

To study the *in vivo* effect of ICAM-1 blockade on VEGF-induced retinal vascular permeability and leukostasis, a well characterized rat ICAM-1 neutralizing monoclonal antibody (mAb) was used (1A29; R&D Systems, Minneapolis, MN).[12–14] The animals were randomly divided into five groups. The first group received no treatment. The second group received 5 μl of phosphate-buffered saline (PBS) injected into the vitreous of the left eye. The third group received 50 ng $VEGF_{165}$ in 5 μl PBS injected into the vitreous of the left eye (12.5 nmol/L final concentration). The fourth group received 50 ng VEGF in PBS injected into the vitreous of the left eye plus 5 mg/kg isotype-matched normal mouse IgG1 (R&D Systems) given intravenously. The fifth group received 50 ng VEGF in PBS injected into the vitreous of the left eye plus 5 mg/kg of the anti-ICAM-1 mAb given intravenously. Twenty-four hours later, retinal leukocyte dynamics and vascular permeability were quantified.

Statistical Analysis

All results are expressed as the mean ± SD. Unpaired groups of two were compared using the two-sample *t*-test or the two-sample *t*-test with Welch's correction. To compare three or more groups, analysis of variance followed by the *post hoc* test with Fisher's protected least signifi-

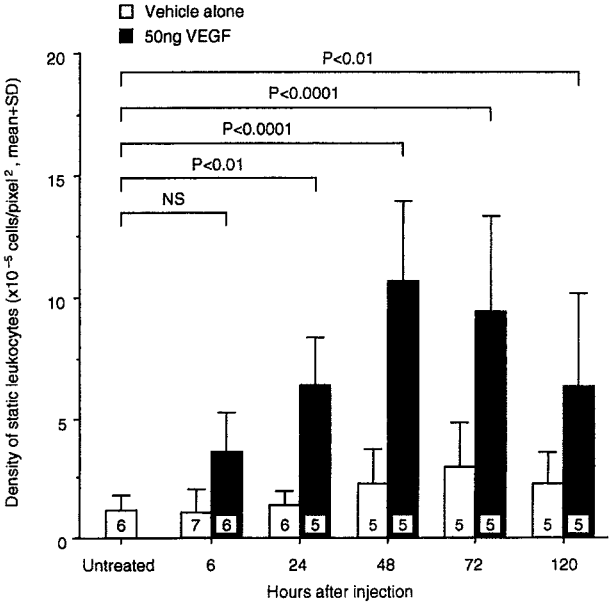

Figure 3. Time course of VEGF-induced retinal leukostasis. Fifty nanograms of VEGF or an equivalent volume of vehicle alone was delivered via intravitreous injection and leukostasis was quantitated with AOLF at the indicated time points.

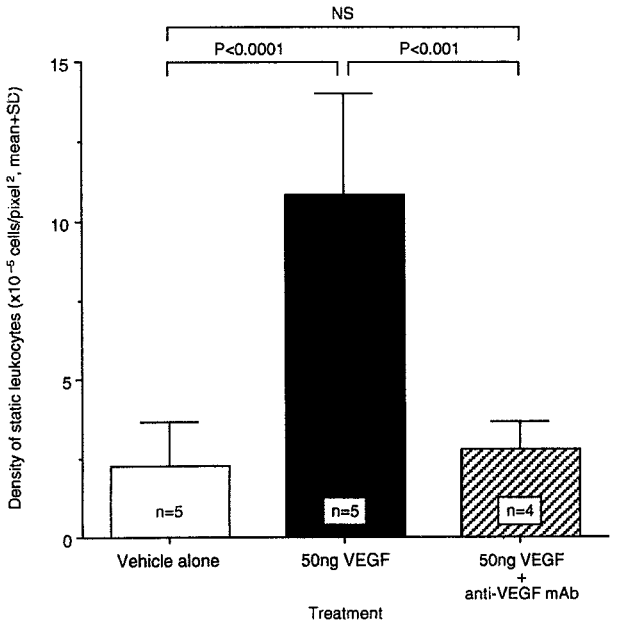

Figure 4. Specificity of VEGF-induced leukostasis. Fifty nanograms of VEGF were delivered intravitreously either alone or combined a 50 molar excess of an anti-VEGF neutralizing mAb (clone A4.6.1). Leukostasis was quantitated with AOLF 48 hours later.

cant difference procedure was used. Differences were considered statistically significant when $P < 0.05$.

Results

VEGF-Induced Retinal Leukostasis

A single 50-ng intravitreous injection of $VEGF_{165}$ (R& D Systems) in 5 μl PBS was able to induce marked retinal leukostasis 48 hours later (Figure 1). Vessel dilation and tortuosity were also evident. A dose-response study demonstrated that a 2.6-fold increase in leukostasis could be induced with as little as 10 ng VEGF (2.5 nmol/L) (Figure 2, $n = 5$, $P < 0.05$). A plateau was reached with 50 to 100 ng VEGF (~4- to 5-fold, $n = 5$, $P = <0.001$ to 0.0001). Based on these data, the 50-ng dose was chosen for the time course experiments. Intravitreous injections of 50 ng VEGF were followed by AOLF 6, 24, 48, 72, and 120 hours later. Twenty-four hours after intravitreous injection, VEGF increased retinal leukostasis 4.8-fold (Figure 3, $n = 5$, $P < 0.01$ *versus* vehicle control). The VEGF-induced leukostasis increases peaked 48 hours postinjection and persisted for at least 120 hours ($n = 5$, $P < 0.01$).

To confirm that this effect was due to VEGF alone, four rats received a mixture of VEGF with a 50:1 molar excess of a previously characterized VEGF-neutralizing monoclonal antibody (A4.6.1, generous gift of Napoleone Ferrara, Genentech, South San Francisco, CA; Figure 4). Co-injection of the anti-VEGF antibody completely abrogated the VEGF-induced leukostasis 48 hours later ($n = 4$, $P < 0.001$).

VEGF-Induced Retinal Capillary Perfusion

Fluorescein angiography performed 20 minutes after AOLF revealed relatively large areas of downstream capillary nonperfusion associated with some of the static leukocytes (Figure 5). The majority of the leukocytes observed appeared to be in the intravascular space. Normal and vehicle-injected eyes did not exhibit nonperfusion (data not shown).

VEGF-Induced Retinal ICAM-1 Gene Expression

Twenty hours after intravitreous injection of 50 ng VEGF or PBS vehicle alone, total RNA was isolated from each rat retina and ICAM-1 gene expression was quantitated using the ribonuclease protection assay (Figure 6A). When normalized to 18S, retinal ICAM-1 levels in the VEGF-injected eyes were 2.8-fold greater than in the eyes injected with vehicle alone (Figure 6B, $n = 5$, $P < 0.02$).

ICAM-1 Blockade of VEGF-Induced Vascular Permeability and Leukostasis

Animals receiving intravitreous VEGF had a 3.2-fold increase in vascular permeabilty 24 hours after injection

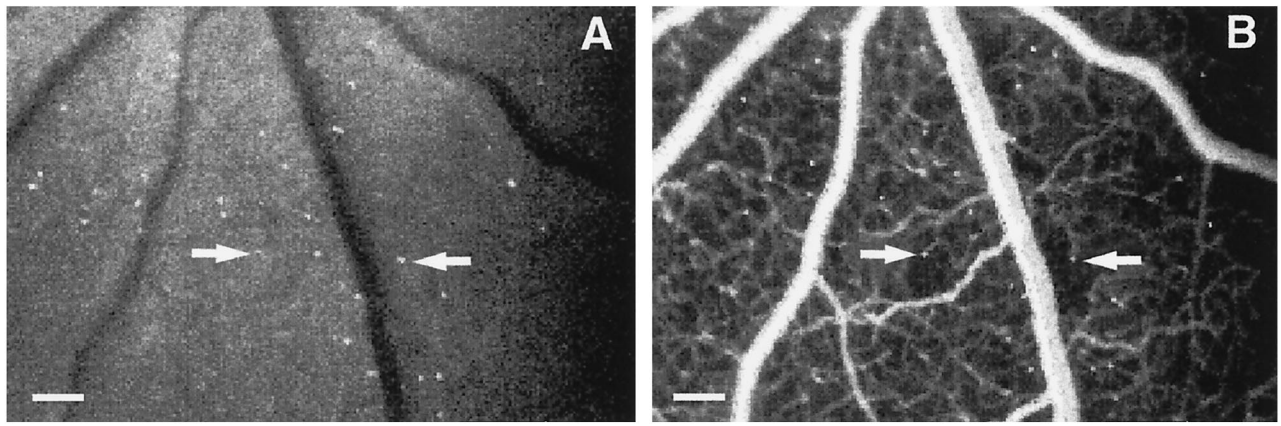

Figure 5. Leukocyte-induced capillary nonperfusion. **A:** Fifty nanograms of VEGF were delivered via intravitreous injection and AOLF was performed 48 hours later. **B:** AOLF was immediately followed by fluorescein angiography and showed areas of capillary nonperfusion downstream from static leukocytes (**arrows**). Scale bar, 100 μm (3.2 pixels = 1 μm).

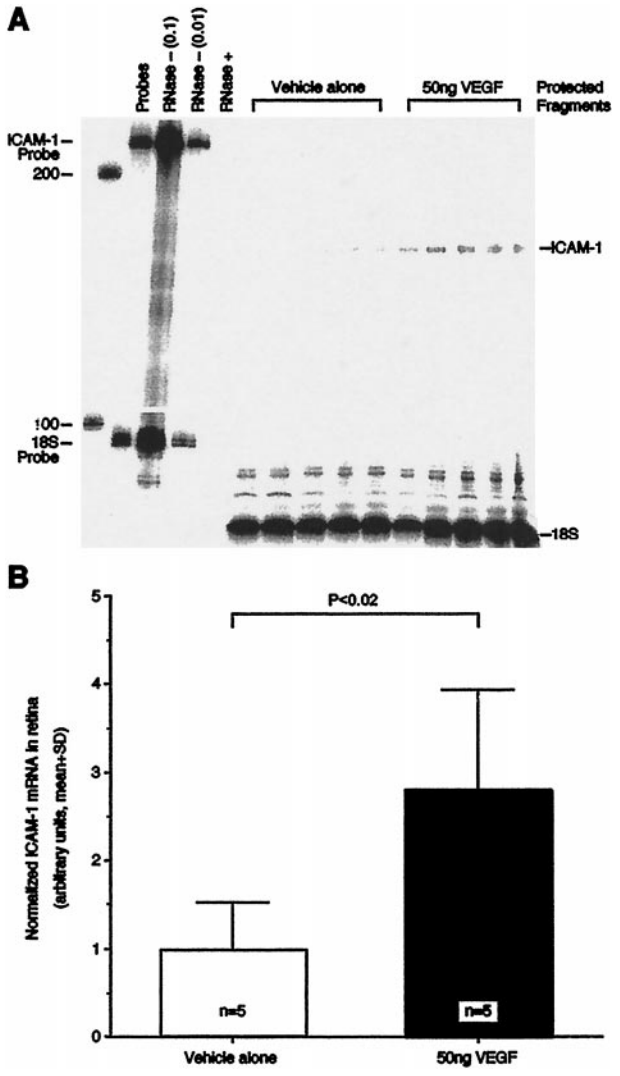

Figure 6. VEGF-induced retinal ICAM-1 gene expression. **A:** The ribonuclease protection assay demonstrated that retinal ICAM-1 levels were significantly increased 20 hours after the intravitreous delivery of 50 ng VEGF. Control animals received 5 μl of PBS solvent alone. Each lane shows the signal from one retina of one animal. The lane labeled "Probes" shows a 100-fold dilution of the full-length ICAM-1 and 18S riboprobes. The lanes labeled "RNase− (0.1)" and "RNase− (0.01)" show the 10-fold and 100-fold dilutions, respectively, of the full-length riboprobes without sample or RNase. The lane labeled "RNase+" shows the full-length riboprobes with RNase, but without sample. **B:** ICAM-1 protection assay data normalized to 18S signal.

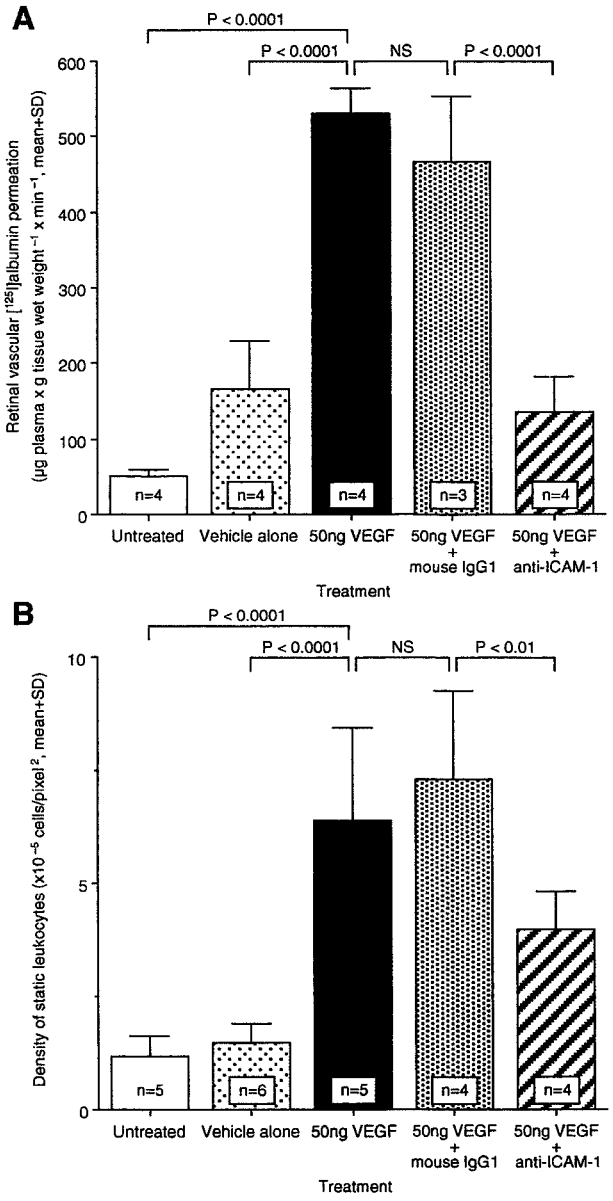

Figure 7. Effect of anti-ICAM-1 mAb on permeability and leukostasis after intravitreous VEGF injection. ICAM-1 bioactivity was inhibited via intravenous administration of ICAM-1 neutralizing antibody, and retinal permeability (**A**) or leukostasis (**B**) were evaluated, respectively. NS, not significant.

(Figure 7A, $n = 4$, $P < 0.0001$ *versus* vehicle control). Similarly, there was a 4.3-fold increase in retinal leukostasis (Figure 7B, $n = 5$, $P < 0.0001$ *versus* vehicle control). Intravenous treatment with the nonimmune control antibody did not significantly alter the degree of VEGF-induced permeability (Figure 7A, $n = 3$, $P > 0.05$) or leukostasis (Figure 7B, $n = 4$, $P > 0.05$). However, the animals receiving intravenous anti-ICAM mAb had a 79% reduction in VEGF-induced retinal vascular permeability (Figure 7A, $n = 4$, $P < 0.0001$ *versus* untreated) and a 54% reduction in VEGF-induced retinal leukostasis (Figure 7B, $n = 4$, $P < 0.01$ *versus* untreated).

Discussion

We have shown that VEGF induces retinal vascular permeability and leukostasis, in part, through ICAM-1. Retinal leukostasis was also spatially linked to capillary nonperfusion. The vitreous concentration at which VEGF begins to induce these changes (12.5 nmol/L) is within the range of vitreous VEGF concentrations observed in human eyes with diabetic retinopathy.[15–17] The leukostasis observed in these studies was specific to VEGF because co-injection of a neutralizing antibody abrogated the response. Finally, these findings are consistent with our work showing VEGF-induced ICAM-1 expression in the retinal vasculature.[8]

Leukocyte adhesion secondary to VEGF has been previously demonstrated in the microvasculature of growing tumors,[18] the corneas of rabbits,[19] and the skin of transgenic mice.[20] Detmar and associates expressed VEGF using the keratin 14 promoter and observed the induction of a vascular cell adhesion molecule-1 (VCAM-1)-mediated leukostasis in the dermis.[20] In a separate study, Melder and associates demonstrated VEGF-induced leukocyte adhesion to tumor vasculature via ICAM-1 and VCAM-1.[18] A tissue-specific heterogeneity for the mediating adhesion molecules may exist, as the Detmar study showed that ICAM-1 inhibition did not affect VEGF-induced skin leukostasis.[18] The present data extend these observations by suggesting that VEGF-induced leukostasis is not an epiphenomenon, as the process is linked to capillary nonperfusion and increased vascular permeability.

At least two mechanisms may be operative in the generation of VEGF-induced vascular permeability. Previous reports have shown that leukocyte-endothelial interactions can trigger endothelial cell adherens and tight junction disorganization,[21,22] as well as increases in vascular permeability.[23] Others have demonstrated that VEGF has direct effects on vascular permeability.[24] *In vitro* studies have documented changes in electrical resistance and hydraulic conductivity in isolated endothelial monolayers treated with VEGF.[24] Risau and coworkers were able to induce fenestrations in VEGF-treated endothelial-epithelial cell cocultures,[25] extending the *in vivo* observations of Roberts and Palade.[26,27] These various mechanisms, although distinct, are not likely to be mutually exclusive. Leukocytes, via their own VEGF, may indirectly serve to amplify the direct effects of VEGF when they bind to endothelium. VEGF has been demonstrated in neutrophils,[28] monocytes,[29] eosinophils,[30] lymphocytes,[31] and platelets.[32] The fact that some leukocytes possess high affinity VEGF receptors and migrate in response to VEGF[33] makes this scenario more likely.

The data also show that VEGF-induced capillary nonperfusion occurs downstream from areas of leukocyte adhesion. Leukocyte-mediated nonperfusion characterizes experimental diabetic retinopathy.[1] In diabetes, patent capillaries become occluded downstream from newly arrived static leukocytes. Later, after the disappearance of the leukocytes, the capillaries reopen. Because neutrophil and monocyte diameters can exceed those of retinal capillary lumens,[34] leukocyte-mediated flow impedance is a likely mechanism. Whether the degree of VEGF-induced nonperfusion is sufficient to trigger retinal hypoxia, a major inducer of VEGF gene expression, remains unknown. Similarly, it is not known if the VEGF-induced leukostasis leads to capillary death, producing the acellular capillaries that characterize diabetic retinopathy. However, these possibilities seem likely and are under investigation.

Taken together, the current findings indicate that VEGF-induced vascular permeability is mediated, in part, by ICAM-1-mediated retinal leukostasis. This mechanism may be unique to the retina, as others have recently demonstrated that VEGF can inhibit leukocyte-endothelium interactions in the rat mesenteric circulation.[35] These data are the first to show that a nonendothelial cell type can contribute to VEGF-induced vascular permeability. They are also the first to provide a mechanism for the retinal capillary nonperfusion induced by VEGF. Given these findings, targeting ICAM-1 may prove useful in the treatment of diseases characterized by VEGF-induced vascular changes, such as diabetic retinopathy.

References

1. Miyamoto K, Khosrof S, Bursell S-E, Rohan R, Murata T, Clermon A, Aiello, LP, Ogura Y, Adamis AP: Prevention of leukostasis and vascular leakage in streptozotocin-induced diabetic retinopathy via intercellular adhesion molecule-1 inhibition. Proc Natl Acad Sci USA 1999, 96:10836–10841
2. Tolentino MJ, Miller JW, Gragoudas ES, Jakobiec FA, Flynn E, Chatzistefanou K, Ferrara N, Adamis AP: Intravitreal injections of vascular endothelial growth factor produce retinal ischemia and microangiopathy in an adult primate. Ophthalmology 1996, 103:1820–1828
3. Okamoto N, Tobe T, Hacket SF, Ozaki H, Vinores M.A, LaRochelle W, Zack D J, Campochiaro PA: Transgenic mice with increased expression of vascular endothelial growth factor in the retina: a new model of intraretinal and subretinal neovascularization. Am J Pathol 1997, 151: 281–291
4. Aiello LP, Bursell SE, Clermont A, Duh E, Ishii H, Takagi C, Mori F, Ciulla TA, Ways K, Jirousek M, Smith LE, King GL: Vascular endothelial growth factor-induced retinal permeability is mediated by protein kinase C in vivo and suppressed by an orally effective beta-isoform-selective inhibitor. Diabetes 1997, 46:1473–1480
5. McLeod DS, Lefer DJ, Merges C, Lutty GA: Enhanced expression of intracellular adhesion molecule-1 and P-selectin in the diabetic human retina and choroid. Am J Pathol 1995, 147:642–653
6. Pe'er J, Folberg R, Itin A, Gnessin H, Hemo I, Keshet E: Upregulated expression of vascular endothelial growth factor in proliferative diabetic retinopathy. Br J Ophthalmol 1996, 80:241–245
7. Murata T, Ishibashi T, Khalil A, Hata Y, Yoshikawa H, Inomata H: Vascular endothelial growth factor plays a role in hyperpermeability of diabetic retinal vessels. Ophthalmic Res 1995, 27:48–52
8. Lu M, Perez V, Ma N, Miyamoto K, Peng HB, Liao JK, Adamis AP: VEGF increases retinal vascular ICAM-1 expression in vivo. Invest Opthalmol Vis Sci 1999, 40:1808–1812
9. Nishiwaki H, Ogura Y, Kimura H, Kiryu J, Miyamoto K, Matsuda N: Visualization and quantitative analysis of leukocyte dynamics in retinal microcirculation of rats. Invest Ophthalmol Vis Sci 1996, 37:1341–1347
10. Miyamoto K, Hiroshiba N, Tsujikawa A, Ogura Y: In vivo demonstration of increased leukocyte entrapment in retinal microcirculation of diabetic rats. Invest Ophthalmol Vis Sci 1998, 39:2190–2194
11. Tilton RG, Kawamura T, Chang KC, Ido Y, Bjercke RJ, Stephan CC, Brock TA, Williamson JR: Vascular dysfunction induced by elevated glucose levels in rats is mediated by vascular endothelial growth factor. J Clin Invest 1997, 99:2192–2202
12. Tamatani T, Miyasaka M: Identification of monoclonal antibodies reactive with the rat homolog of ICAM-1, and evidence for a differential involvement of ICAM-1 in the adherence of resting versus activated lymphocytes to high endothelial cells. Int Immunol 1990, 2:165–171
13. Kawasaki K, Yaoita E, Yamamoto T, Tamatani T, Miyasaka M, Kihara I: Antibodies against intercellular adhesion molecule-1 and lymphocyte function-associated antigen-1 prevent glomerular injury in rat experimental crescentic glomerulonephritis. J Immunol 1993, 150: 1074–1083
14. Kelly KJ, Williams WW, Colvin RB, Bonventre JV: Antibody to intercellular adhesion molecule-1 protects the kidney against ischemic injury. Proc Natl Acad Sci USA 1994, 91:812–816
15. Adamis AP, Miller J, Bernal M-T, D'Amico DJ, Folkman J, Yeo T-K, Yeo K-T: Increased vascular endothelial growth factor levels in the vitreous of eyes with proliferative diabetic retinopathy. Am J Ophthalmol 1994, 118:445–450
16. Aiello LP, Avery RL, Arrigg PG, Keyt BA, Jampel HD, Shah ST, Pasquale LR, Thieme H, Iwamoto MA, Park JE, Nguyen HV, Ferrara N, King GL: Vascular endothelial growth factor in ocular fluid of patients

with diabetic retinopathy and other retinal disorders. N Engl J Med 1994, 331:1480–1487
17. Malecaze F, Clamens S, Simorre-Pinatel V, Chollet P, Favard C, Bayard F, Plouet J: Detection of vascular endothelial growth factor messanger RNA and vascular endothelial growth factor-like activity in proliferative diabetic retinopathy. Arch Ophthalmol 1994, 112:1476–1482
18. Melder RJ, Koenig GC, Witwer BP, Safabakhsh N, Munn LL, Jain RK: During angiogenesis, vascular endothelial growth factor and basic fibroblast growth factor regulate natural killer cell adhesion to tumor endothelium. Nat Med 1996, 2:992–997
19. Becker MD, Kruse FE, Azzam L, Nobiling R, Reichling J, Volcker HE: In vivo significance of ICAM-1-dependent leukocyte adhesion in early corneal angiogenesis. Invest Ophthalmol Vis Sci 1999, 40:612–618
20. Detmar M, Brown LF, Schon MP, Elicker BM, Velasco P, Richard L, Fukamura D, Monsky D, Claffey KP, Jain RK: Increased microvascular density and enhanced leukocyte rolling and adhsion in the skin of VEGF transgenic mice. J Invest Dermatol 1998, 111:1–6
21. Del Maschio A, Zanetti A, Corada M, Rival Y, Ruco L, Lampugnani MG, Dejana E: Polymorphonuclear leukocyte adhesion triggers the disorganization of endothelial cell-to-cell adherens junctions. J Cell Biol 1996, 135:497–510
22. Bolton SJ, Anthony DC, Perry VH: Loss of tight junction proteins occludin and zonula occludens-1 from cerebral vascular endothelium during neutrophil-induced blood-brain barrier breakdown in vivo. Neuroscience 1998, 86:1245–1257
23. Kurose I, Anderson DC, Miyasaka M, Tamatani T, Paulson JC, Todd RF, Rusche JR, Granger DN: Molecular determinants of reperfusion-induced leukocyte adhesion and vascular protein leakage. Circ Res 1994, 74:336–343
24. Yaccino JA, Chang YS, Hollis TM, Gardner TW, Tarbell JM: Physiological transport properties of cultured retinal microvascular endothelial cell monolayers. Curr Eye Res 1997, 16:761–768
25. Esser S, Wolburg K, Wolburg H, Breier G, Kurzchalia T, Risau W: Vascular endothelial growth factor induces endothelial fenestrations in vitro. J Cell Biol 1998, 140:947–959
26. Roberts WG, Palade GE: Increased microvascular permeability and endothelial fenestration induced by vascular endothelial growth factor. J Cell Sci 1995, 108:2369–2379
27. Roberts WG, Palade GE: Neovasculature induced by vascular endothelial growth factor is fenestrated. Cancer Res 1997, 57:765–772
28. Gaudry M, Bregerie O, Andrieu V, El Benna J, Pocidalo MA, Hakim J: Intracellular pool of vascular endothelial growth factor in human neutrophils. Blood 1997, 41:4153–4161
29. Iijima K, Yoshikawa N, Connolly DT, Nakamura H: Human mesangial cells and peripheral blood mononuclear cells produce vascular permeability factor. Kidney Int 1993, 44:959–966
30. Horiuchi T, Weller PF: Expression of vascular endothelial growth factor by human eosinophils: upregulation by granulocyte macrophage colony-stimulating factor and interleukin-5. Am J Respir Cell Mol Biol 1997, 17:70–77
31. Freeman MR, Schneck FX, Gagnon ML, Corless C, Soker S, Niknejad K, Peoples GE, Klagsbrun M: Peripheral blood T lymphocytes and lymphocytes infiltrating human cancers express vascular endothelial growth factor: a potential role for T cells in angiogenesis. Cancer Res 1995, 55:4140–4145
32. Mohle R, Green D, Moore MA, Nachman RL, Rafii S: Constitutive production and thrombin-induced release of vascular endothelial growth factor by human megakaryocytes and platelets. Proc Natl Acad Sci USA 1997, 94:663–668
33. Shen H, Clauss M, Ryan J, Schmidt AM, Tijburg P, Borden L, Connolly D, Stern D, Kao J: Characterization of vascular permeability factor/vascular endothelial growth factor receptors on mononuclear phagocytes. Blood 1993, 81:2767–2773
34. Schroder S, Palinski W, Schmid-Schonbein GW: Activated monocytes and granulocytes, capillary nonperfusion, and neovascularization in diabetic retinopathy. Am J Pathol 1991, 139:81–100
35. Scalia R, Booth G, Lefer DJ: Vascular endothelial growth factor attenuates leukocyte-endothelium interaction during acute endothelial dysfunction: essential role of endothelium-derived nitric oxide. FASEB J 1999, 9:1039–1046